Dynamic Simulation of an Oxygen-Hydrogen Combustion Turbine System Using Modelica

Yutaka Watanabe Toru Takahashi Kojun Suzuki

Central Research Institute of Electric Power Industry, Japan, {yutaka,toru-tak,s-kojun}@criepi.denken.or.jp

Abstract

Introducing hydrogen power generation in the power industry may contribute to achieve carbon neutrality by 2050. Hydrogen mixed-fuel gas turbines are available, and pure hydrogen-fueled gas turbines are being developed. Meanwhile, power generation systems based on oxygen–hydrogen combustion turbines have been devised. Such system uses hydrogen as fuel and oxygen as oxidizer, yielding only water vapor as the byproduct of combustion. In addition, as the system performs a semi-closed cycle involving the Brayton and Rankine cycles, high efficient zero-emission power generation is expected with higher thermal efficiency than that of the combined cycle in conventional gas turbines. Basic technologies for oxygen-hydrogen combustion turbines in power generation systems are being developed in Japan as part of the research and development at NEDO for hydrogen utilization. In this study, a dynamic model of the entire system for a 1400 °C-class rationalization system was constructed using a Modelica-based tool developed by the Central Research Institute of Electric Power Industry, Japan. The dynamic behavior considering preliminary load following control was then characterized based on simulation results.

Keywords: Closed cycle, Hydrogen, Dynamic simulation, Load following

Nomenclature

A	flow area [m^2]
K	heat transfer coefficient [$kW/(m^2 \cdot K)$]
cp	heat capacity [$kW/(kg \cdot K)$]
F	mass flow rate [kg/s]
H	specific enthalpy [kJ/kg]
LHV/HHV	lower/higher heating value [kJ/kg]
k	specific heat ratio [-]
M	mass [kg]
Q	heat transfer rate [kJ/s]
P	pressure [MPa]
v	specific volume [m^3/kg]
W	power [kW]
η	adiabatic efficiency [-]

Subscripts

ad	adiabatic change
c	cold flow
cb	combustion
cp	compressor
f	fuel
h	hot flow
i	inlet
j	segment number
m	metal
o	outlet
st	steam turbine

1 Introduction

To address climate change, actions toward decarbonization and net-zero CO2 emissions in the global energy sector must be implemented by 2050 (IEA, 2021). A carbon-neutral society will widely use hydrogen. Thus, hydrogen supply infrastructures and power generation systems are being increasingly demanded. Fuel cells are a well-known power generation method using hydrogen, but gas turbines (GTs) are more suitable for large-scale power generation. The impact of CO2 reduction will be significant if hydrogen is used at large-scale electric power generation plants. Currently, hydrogen mixed-fuel GTs are available, and pure hydrogen-fueled GTs are expected to be developed by 2030 (ETN, 2021). Meanwhile, a power generation system based on oxygen-hydrogen combustion turbines that perform direct combustion of these gases has been devised, seeming promising for high-efficiency hydrogen power generation. In this system, the sole byproduct of combustion at a very high temperature is water vapor if hydrogen and oxygen are combusted at the theoretically compatible ratio. As the conventional Rankine cycle is intended for external combustion engines, it is difficult

to achieve higher temperatures than those in GTs, which perform internal combustion, owing to limitations in the heat resistance of heat transfer tubes in the boiler. In addition, in a conventional GT, the amount of generated NOx increases with increasing temperature. In contrast, in oxygen-hydrogen combustion, NOx generation is prevented owing to the absence of nitrogen in the reaction gas. Therefore, oxygen-hydrogen combustion turbines may be suitable for both combustion at higher temperatures and highly efficient zero-emission power generation. Hence, they may achieve higher power generation efficiency than conventional GTs with a combined cycle.

Oxygen-hydrogen closed cycles and their system parameter optimization have been widely studied, leading to systems such as those based on the Graz cycle (Sanz et al., 2018), a new Rankine cycle (Fukuda and Dozono, 2000; Soufi et al., 2004; Bannister et al., 1998; Schouten and Klein, 2020), and even topping with a fuel cell (Millewski, 2015). In Japan, the WE-NET project (Mitsugi et al., 1998) was conducted between 1993 and 1998 to achieve an efficiency above 60% (HHV) (approximately 71% regarding LHV) at a turbine inlet temperature of 1700 °C. A topping regeneration cycle and new Rankine cycle were proposed, demonstrating that the target efficiency could be achieved through optimization (Sugisita et al., 1998).

Since 2018, the development of basic technology for a power generation system based on oxygen-hydrogen combustion turbines is underway as part of a research and development project at the New Energy and Industrial Technology Development Organization (NEDO) for leading hydrogen utilization (NEDO, 2022). By 2020, the oxygen-hydrogen combustion power generation was reviewed considering the knowledge obtained from the WE-NET project, and a parameter study of the turbine inlet conditions (i.e., steam pressure and temperature) for achieving 75% (LHV) thermal efficiency was conducted using the Graz cycle. Simultaneously, a system that leverages the cycle by rationalizing the factors that increase costs while minimizing the decrease in thermal efficiency was investigated, leading to identify technical research problems to be addressed for obtaining a high-efficiency system. Technical studies on rationalization systems are being conducted based on results from the abovementioned pioneering studies.

Despite the advancements, most studies on oxygen-hydrogen combustion turbine cycles have been focused on the optimization of the cycle configuration and system performance. Such studies have demonstrated the possibility of achieving high efficiency, but few studies on operational characteristics such as start-up, shutdown, and load change are available, with an exception being a study on the start-up operation of the new Rankine cycle (Funatsu et al., 1998). When variable renewable energies are introduced into the power system in large quantities in the future, power generation systems are expected to have more opportunities to operate at partial load. Therefore, in addition to their rated performance, their operability should be evaluated. In fact, determining the dependence of the system performance on different load changes is important. For example, condensate generation, rapid temperature fluctuation, and excess temperature may occur during partial load operation. Hence, a system-level dynamic model should be established. Physical modeling is especially useful to predict both the dynamic behavior and off-design conditions for the entire operational range of a power generation system. In addition, the model is important for efficient development, prediction, and evaluation of operational characteristics of the entire system at the conceptual stage as well as understanding operational problems and specifications for components at an early stage. Although many analyses of thermal power generation systems have been performed using Modelica, few have been performed considering oxygen-hydrogen combustion turbines.

To evaluate the dynamic performance under load changes and capture the general behavior of the target system, we constructed a dynamic model of an oxygen-hydrogen combustion turbine system using a Modelica-based tool developed by the Central Research Institute of Electric Power Industry, Japan. Then, simple load following control was implemented, and the dynamic behavior was evaluated based on the corresponding simulation results.

2 Methods

2.1 System Configuration

Figure 1 shows a diagram of the system considered in this study, while Figure 2 shows the temperature–entropy diagram, and Table 1 lists the main performance parameters of the system. Although the system was based on the Graz cycle, it was intended to leverage the benefits of the cycle by omitting the high-pressure turbine and streamlining equipment specifications that increase manufacturing costs by using a combustion temperature of 1400 °C. Therefore, the system mainly comprises a combustor, high-temperature turbine (HTT), compressor, waste heat recovery boiler (HRSG), constant pressure steam turbine (LPT), condenser, and feedwater pump. When hydrogen and oxygen completely react in compatible quantities in the combustor, the only working fluid and combustion product is steam, and the system is characterized by a combined cycle configuration involving the high-temperature Brayton cycle and low-temperature Rankine cycle. The steam circulates in the system as the working fluid, and the water produced during combustion is discharged via a drain after passing through the condenser.

DOI
10.3384/ecp19315

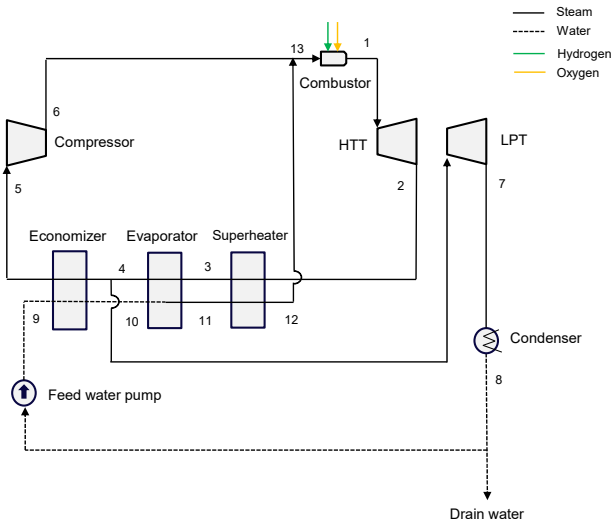

Figure 1. Schematic of target power generation system.

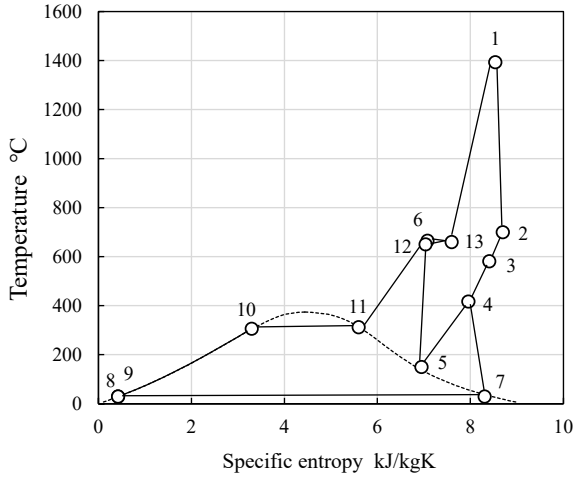

Figure 2. Temperature-entropy diagram of target power generation system.

Table 1. Main performance parameters of target power generation system.

Parameter	*Value*
Power output	102.3 MW
Thermal efficiency	68.3 %LHV
Combustion temperature	1393 °C
HTT inlet pressure	10.0 MPa

2.2 The Dynamic Model

A dynamic model of the system was established using the Modelica-based tool developed by the Central Research Institute of Electric Power Industry (Watanabe et al., 2017). The system model was constructed by

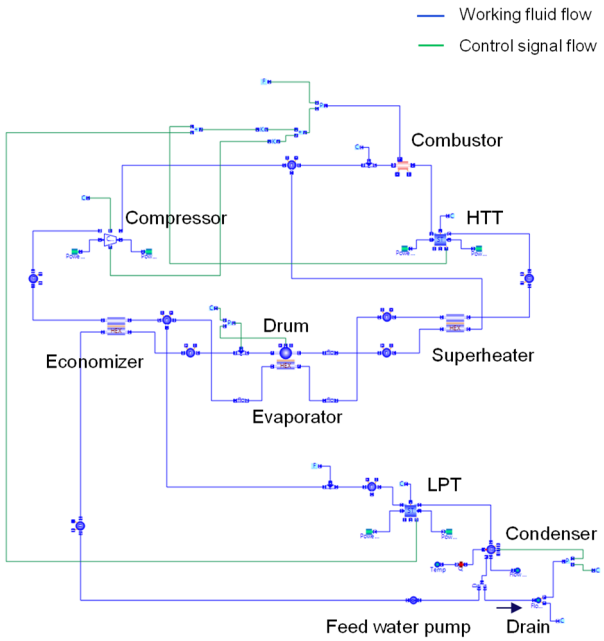

Figure 3. Overview of dynamic model.

combining static and dynamic component models and controllers, as shown in Figure 3. The SimulationX software was used for simulations.

We assume that hydrogen and oxygen are combusted in compatible proportions and that the working fluid contains no components other than water. In addition, the effects of residual oxygen and hydrogen are neglected.

2.2.1 Combustor

The equation of the combustion reaction is given by

$$2H_2 + O_2 \rightarrow 2H_2O \quad (1)$$

The combustion is assumed to be instantaneous, and the heat generated is calculated statically from the calorific value of the fuel (hydrogen) as follows:

$$Q_{\mathrm{f}} = HHV_{\mathrm{f}} \cdot F_{\mathrm{f}} \quad (2)$$

The combustion components are also calculated statically. The hydrogen flow rate is set as an input condition, and the oxygen flow rate depends on the hydrogen flow rate to meet the conditions for combustion at an equivalent ratio of 1.0. The combustion products are water vapor, and the amount of production is given by

$$F_{\mathrm{H20,cb}} = F_{\mathrm{H2}} + F_{\mathrm{O2}} \quad (3)$$

The pressure and temperature are calculated for the dynamics of the volume model assuming that the fuel gas enters a vessel of constant volume. A diagram of the Modelica model is shown in Figure 4.

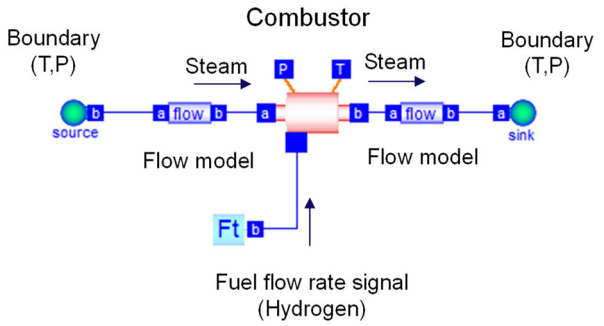

Figure 4. Diagram for calculations of combustor model.

2.2.2 Steam Compressor

The steam compressor is also modeled in the static mode. The specific enthalpy at the turbine outlet and power output are respectively given by

$$H_{\mathrm{o}} = H_{\mathrm{i}} + \frac{H_{\mathrm{o,ad}} - H_{\mathrm{i}}}{\eta_{\mathrm{cp}}} \tag{4}$$

$$W_{\mathrm{cp}} = F_{\mathrm{cp}}(H_{\mathrm{o}} - H_{\mathrm{i}}) \tag{5}$$

As the design of the steam compressor is not complete, a simple functional relation between the adiabatic efficiency and mass flow rate is assumed. The compressor flow is approximated based on the appropriate compressor map in terms of pressure ratio, rotation speed, and opening degree of the inlet guide vane.

2.2.3 Steam Turbine

HTTs and LPTs are described by static models. The enthalpy at the turbine outlet and power output are respectively given by

$$H_{\mathrm{o}} = H_{\mathrm{i}} - \eta_{\mathrm{st}}(H_{\mathrm{i}} - H_{\mathrm{o,ad}}) \tag{6}$$

$$W_{\mathrm{st}} = F_{\mathrm{st}}(H_{\mathrm{o}} - H_{\mathrm{i}}) \tag{7}$$

As the steam turbine is not completely designed, a simple functional relation between the adiabatic efficiency and mass flow rate is assumed. The steam flow rate is calculated using the nozzle flow equation:

$$G_{\mathrm{st}} = \begin{cases} A\sqrt{2\frac{k}{k-1}\frac{P_{\mathrm{i}}}{v_{\mathrm{i}}}\left[\left(\frac{P_{\mathrm{o}}}{P_{\mathrm{i}}}\right)^{\frac{2}{k}} - \left(\frac{P_{\mathrm{o}}}{P_{\mathrm{i}}}\right)^{\frac{k+1}{k}}\right]}, & \left(\frac{P_{\mathrm{o}}}{P_{\mathrm{i}}} \geq \left(\frac{2}{k+1}\right)^{\frac{k}{k-1}}\right) \\ A\sqrt{k\left(\frac{2}{k+1}\right)^{\frac{k+1}{k-1}}\frac{P_{\mathrm{i}}}{v_{\mathrm{i}}}}, & \left(\frac{P_{\mathrm{o}}}{P_{\mathrm{i}}} \leq \left(\frac{2}{k+1}\right)^{\frac{k}{k-1}}\right) \end{cases} \tag{8}$$

2.2.4 Heat Exchanger

For the superheater and economizer, finite volume models divided along the vertical direction are used, as illustrated in Figure 5. The effects of mass and energy conservation laws are given by Eqs. (9)-(13), and the heat transfer equations are given by Eqs. (14) and (15).

$$\frac{d}{dt}M_{\mathrm{h},j} = F_{\mathrm{h},j-1} - F_{\mathrm{h},j} \tag{9}$$

$$\frac{d}{dt}M_{\mathrm{c},j} = F_{\mathrm{c},j+1} - F_{\mathrm{c},j} \tag{10}$$

$$\frac{d}{dt}\left(M_{\mathrm{h},j}H_{\mathrm{h},j}\right) = F_{\mathrm{h},j-1}\left(H_{\mathrm{h},j-1} - H_{\mathrm{h},j}\right) - Q_{\mathrm{h},j} \tag{11}$$

$$\frac{d}{dt}\left(M_{\mathrm{c},j}H_{\mathrm{c},j}\right) = F_{\mathrm{c},j+1}\left(H_{\mathrm{c},j+1} - H_{\mathrm{c},j}\right) + Q_{\mathrm{c},j} \tag{12}$$

$$cp_{\mathrm{m},j}M_{\mathrm{m},j}\frac{d}{dt}T_{\mathrm{m},j} = Q_{\mathrm{h},j} - Q_{c,j} \tag{13}$$

$$Q_{\mathrm{h},j} = AK_{\mathrm{h},j}\left(T_{\mathrm{h},j} - T_{\mathrm{m},j}\right) \tag{14}$$

$$Q_{\mathrm{c},j} = AK_{\mathrm{c},j}\left(T_{\mathrm{m},j} - T_{\mathrm{c},j}\right) \tag{15}$$

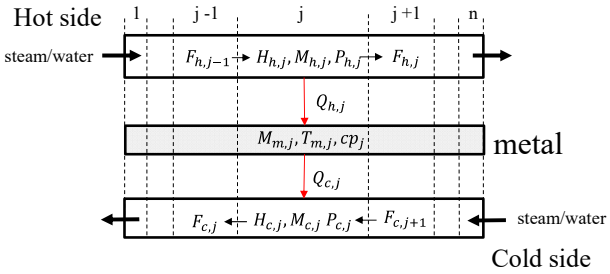

Figure 5. Schematic of finite element heat exchanger model.

The evaporator is modeled as a finite volume model, while the drum is modeled as a pressure vessel element satisfying the two-phase condition. Level control is considered to maintain a constant water level in the drum by adjusting a water supply valve. The heat transfer coefficient is also considered along with the variations at partial load with respect to mass flows.

2.2.5 Condenser

The condenser is modeled as a pressure vessel, where water and steam are mixed in a separated state. Dry or wet vapor enters the inlet and is discharged into water at the outlet. Again, level control is introduced to maintain a constant water level in the condenser and adjust the amount of condensate water by adjusting a drain valve.

To calculate the properties of water and steam in the model, we use the original function model created based on the IAPSW-IF97 formulation (Fernandez-Prini and

DOI
10.3384/ecp19315

Dooley, 1997). The equipment performance parameters are configured based on heat balance and computed results. The weights of the heat transfer metal surface of the heat exchanger and piping volume can also be configured.

2.3 Load Change Strategy

In this study, the fuel flow rate was controlled based on the difference between the desired and computed power outputs, as illustrated in Figure 6. Other possible operating variables included the compressor inlet guide vane and steam governor valves, which were assumed to operate at a constant point.

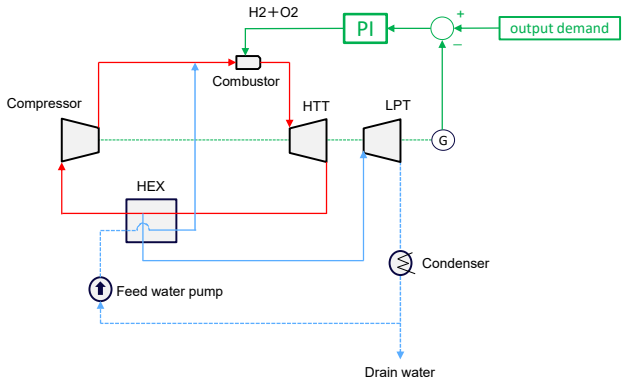

Figure 6. Diagram of load change strategy.

3 Results and Discussion

The system characteristics were examined when the load dropped and increased between 100% and 50%. The simulation input was a load command, and the load change rate was set to 10% per minute. This scenario was set up according to the operational conditions referred to existing and future power generation systems using GTs with combined cycles.

3.1 Load Reduction

Figure 7 shows the simulation results for load reduction. The values for power in figure 7(a) are given relative to the rated power output, and the values in the other figures are given relative to the value of the rated power output. The HTT output followed the load command, while the LPT output changed with a delay attributable to the delayed response of the steam caused by the heat capacity of the heat exchanger. The CP power also changed with a delay for the above reason. The thermal efficiency was lower at partial load than at the rated output. In addition, the fuel flow rate to the GT followed the load command, thereby reducing the combustion temperature, while the turbine outlet temperature showed large fluctuations, and it took time for the system state in the cycle to stabilize. The compressor inlet temperature and pressure also fluctuated, but the compressor inlet state showed less overshooting and fluctuations than the HTT outlet state. This is attributable to both the heat capacity in the heat exchanger and suppression of the effect of short-time fluctuations.

3.2 Load Increase

As shown in Figure 8, the HTT output followed the load command quickly as the fuel flow rate to the GT increased during load increase. On the other hand, the LPT output and CP power changed with a delay, like in the case of load reduction. In addition, the system state at the turbine outlet and compressor inlet fluctuated, and the steam state in the cycle took time to stabilize. Countermeasures (e.g., installing sprays) should be considered to prevent overshooting in parameters such as the temperatures of the combustor inlet steam and HTT outlet steam.

3.3 Problems and Countermeasures for Load Changes

The load change results indicate some sites where the system state considerably fluctuates using this control strategy. Such fluctuations can destabilize plant conditions and increase the heat load on equipment. Therefore, they should be minimized for stable operation through countermeasures taken by changing component specifications and control methods.

To evaluate the effect of the HRSG heat capacity on the system response, simulation results of load following when the heat capacity was set to half of the original were obtained, as shown in Figure 9. The undershoot width of the HTT outlet temperature reduced by decreasing the HRSG heat capacity. This can be attributed to the ratio of the delay in the LPT output being compensated by the reduced GT output, thereby mitigating the change in the fuel flow rate supplied to the GT. Thus, the HRSG specifications are important for system stability under changing load. In addition, other control methods should be considered to reduce fluctuations in the compressor inlet and HTT outlet for stable operation.

4 Conclusion

We established a dynamic model for a power generation system based on oxygen–hydrogen combustion turbines to evaluate its performance and dynamic behavior based on load following control. This study was preliminary and included various assumptions. In future work, we will improve the accuracy of the analytical model by considering the detailed designs of the system components. In addition, we will evaluate other types of load changes.

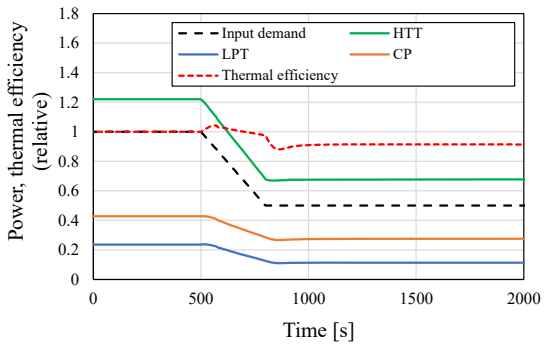

(a) Power output and thermal efficiency

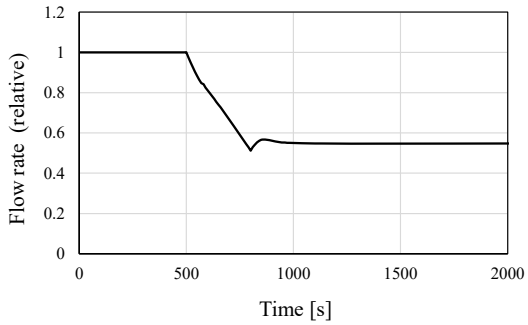

(b) Fuel flow rate

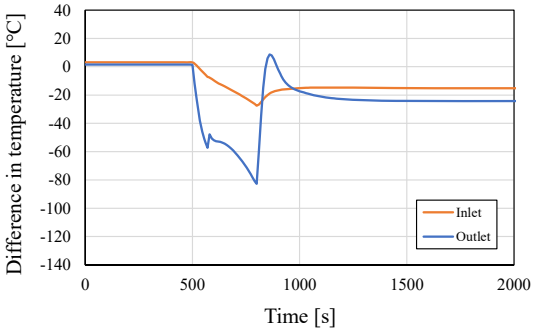

(c) HTT inlet and outlet temperature

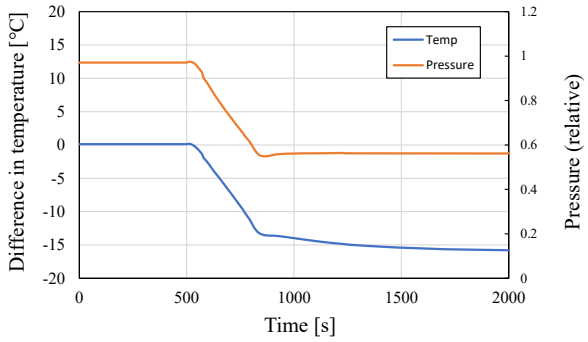

(d) Compressor inlet temperature and pressure

Figure 7. Simulation results during load reduction.

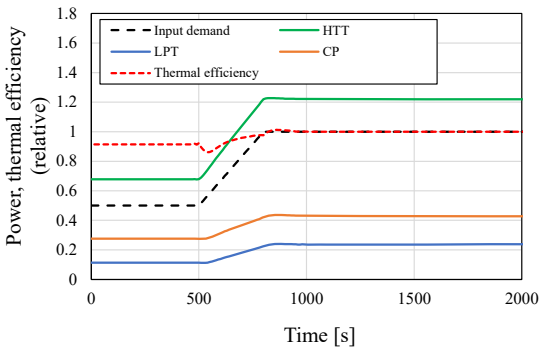

(a) Power output and thermal efficiency

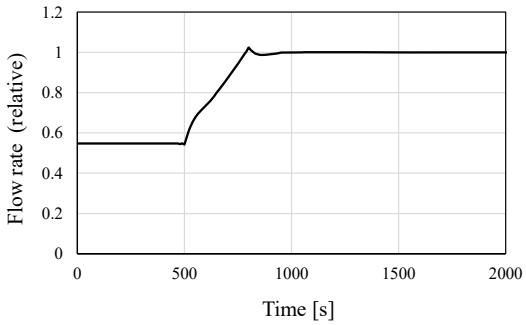

(b) Fuel flow rate

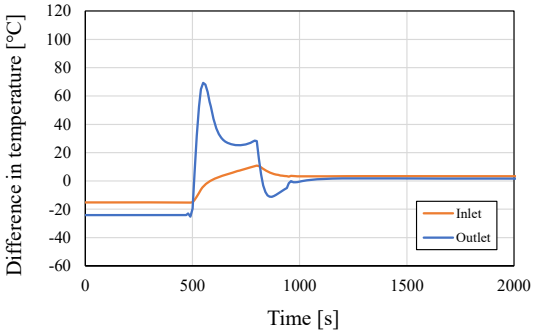

(c) HTT inlet and outlet temperature

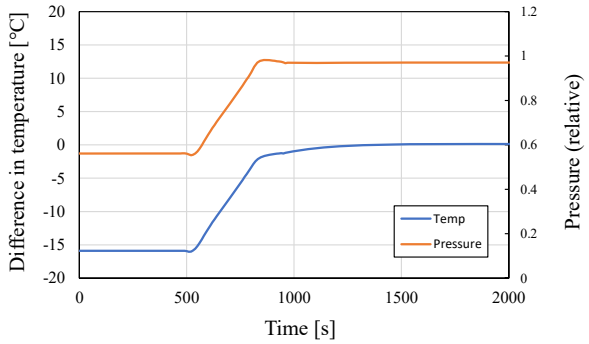

(d) Compressor inlet temperature and pressure

Figure 8. Simulation results during load increase.

DOI
10.3384/ecp19315

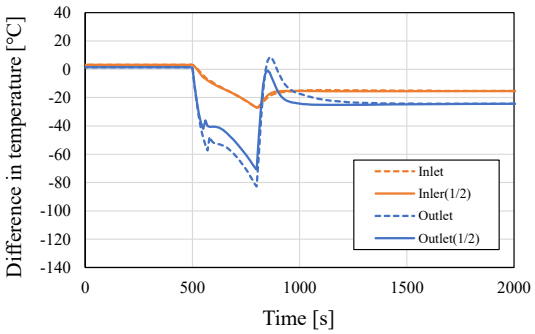

(a) Load reduction

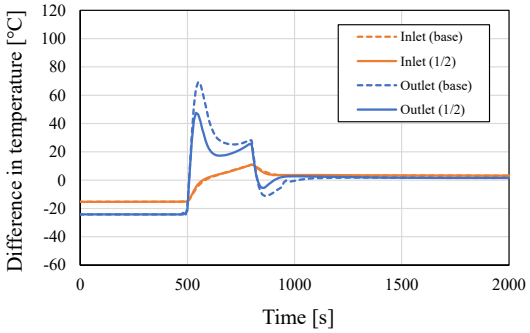

(b) Load increase

Figure 9. Simulation results of HTT inlet and outlet condition

Acknowledgements

This study is based on results obtained from a project, JPNP14021, commissioned by the New Energy and Industrial Technology Development Organization (NEDO).

References

R. L. Bannister, R. A. Newby, and W. C. Yang. Development of a hydrogen-fueled combustion turbine. Journal of Engineering for Gas Turbines and Power, 120(2):276–283, 1998. doi: 10.1115/1.2818116.

ETN. Hydrogen gas turbines. https://etn.global/wp-content/uploads/2020/02/ETN-Hydrogen-Gas-Turbines-report.pdf (accessed: September 5, 2022).

R. Fernandez-Prini and R. B. Dooley. Release on the IAPWS industrial formulation 1997 for the thermodynamic properties of water and steam. The International Association for the Properties Water and Steam, Erlangen, Germany, 1997.

Masafumi Fukuda and Yoshikazu Dozono. Double reheat Rankine cycle for hydrogen-combustion, turbine power plants. Journal of Propulsion and Power, 16(4):562–567, 2000. doi: 10.2514/2.5639.

T. Funatsu, M. Fukuda, and Y. Dohzono. Start up analysis of a H2-O2 fired gas turbine cycle. Proceedings of the ASME 1997 International Gas Turbine and Aeroengine Congress and Exhibition, 97-GT-491, 1997. doi: 10.1115/97-GT-491.

IEA. Net Zero by 2050. https://www.iea.org/reports/net-zero-by-2050 (accessed: September 5, 2022).

Jaroslaw Millewski. Hydrogen utilization by steam turbine cycles. Journal of Power Technologies, 95(4):258–264, 2015.

Chiba Mitsugi, Arai Harumi, and Fukuda Kenzo. WE-NET: Japanese hydrogen program. International Journal of Hydrogen Energy, 23(3):159–165, 1998. doi: 10.1016/S0360-3199(97)00042-6.

NEDO. Advancement of hydrogen technologies and utilizati on project. https://www.nedo.go.jp/english/activities/activities_ZZJP_100068.html (accessed September 5, 2022).

Wolfgang Sanz, Martin Braun, Herbert Jericha, and Max F. P latzer. Adapting the zero-emission Graz Cycle for hydroge n combustion and investigation of its part load behavior. In ternational Journal of Hydrogen Energy, 43(11):5737–574 6, 2018. doi: 10.1016/j.ijhydene.2018.01.162.

Bram Schouten and Sikke Klein. The optimization of hydrogen oxygen cycles. Proceedings of ASME Turbo Expo 2020, GT2020-14592, 2020. doi: 10.1115/GT2020-14592.

Mohammed G. Soufi, Terushige Fujii, Katsumi Sugimoto, and Hitoshi Asano. A new Rankine cycle for hydrogen-fired power generation plants and its exergetic efficiency. International Journal of Exergy, 1(1):29–46, 2004. doi: 10.1504/IJEX.2004.004732.

H. Sugisita, H. Mori, and K. Uematsu. A study of thermodynamic cycle and system configurations of hydrogen combustion turbines. International Journal of Hydrogen Energy, 23(8):705–712, 1998. doi: 10.1016/S0360-3199(97)00081-5.

Yutaka Watanabe, Toru Takahashi, and Masashi Nakamoto. Dynamic simulation of startup characteristics for the advanced humid air turbine system. Proceedings of ASME Turbo Expo 2017, GT2017-64699, 2017. doi: 10.1115/GT2017-64699.